LBL-16703
Preprint c.2

Lawrence Berkeley Laboratory

UNIVERSITY OF CALIFORNIA

Materials & Molecular Research Division

RECEIVED
LAWRENCE
BERKELEY LABORATORY
FEB 1 1984
LIBRARY AND
DOCUMENTS SECTION

Submitted to the Review of Scientific Instruments

FAST, SELF-COMPENSATING SPECTRAL-SCANNING ELLIPSOMETER

R.H. Muller and J.C. Farmer

October 1983

TWO-WEEK LOAN COPY

This is a Library Circulating Copy which may be borrowed for two weeks. For a personal retention copy, call Tech. Info. Division, Ext. 6782.

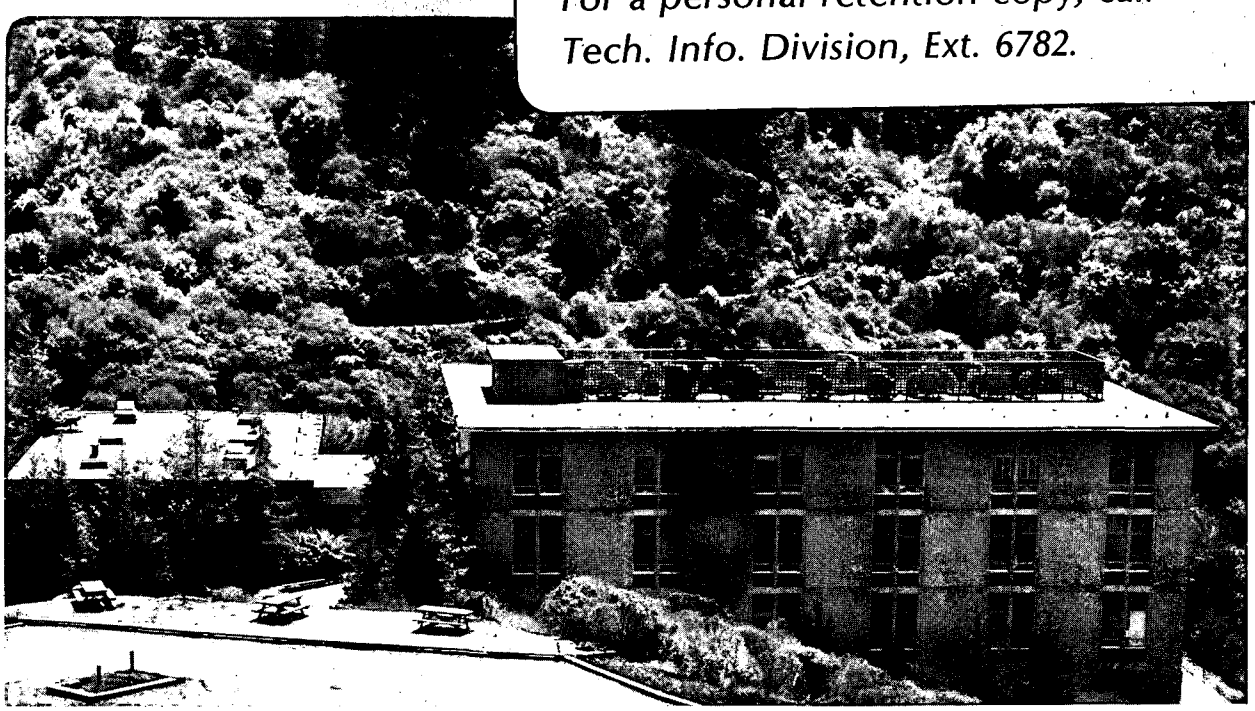

LBL-16703 c.2

Prepared for the U.S. Department of Energy under Contract DE-AC03-76SF00098

DISCLAIMER

This document was prepared as an account of work sponsored by the United States Government. While this document is believed to contain correct information, neither the United States Government nor any agency thereof, nor the Regents of the University of California, nor any of their employees, makes any warranty, express or implied, or assumes any legal responsibility for the accuracy, completeness, or usefulness of any information, apparatus, product, or process disclosed, or represents that its use would not infringe privately owned rights. Reference herein to any specific commercial product, process, or service by its trade name, trademark, manufacturer, or otherwise, does not necessarily constitute or imply its endorsement, recommendation, or favoring by the United States Government or any agency thereof, or the Regents of the University of California. The views and opinions of authors expressed herein do not necessarily state or reflect those of the United States Government or any agency thereof or the Regents of the University of California.

LBL-16703

FAST, SELF-COMPENSATING SPECTRAL-SCANNING ELLIPSOMETER

Rolf H. Muller and Joseph C. Farmer*

Lawrence Berkeley Laboratory
Materials and Molecular Research Division
and
Department of Chemical Engineering
University of California, Berkeley
Berkeley, California, 94720

ABSTRACT

The advantages of rapid spectral scanning have been combined with the inherent accuracy of a compensating ellipsometer operated in the polarizer-compensator-sample-analyzer configuration. Wavelength is scanned over the visible-UV (370-720 nm) at a maximum rate of 114 nm/s by rotating a continuously-variable interference filter. A three-reflection Fresnel rhomb serves as the achromatic quarter-wave compensator. A microcomputer is used to collect spectroscopic measurements, perform instrument calibrations, digital filtering and data interpretation.

*Present address: Sandia Laboratory, Livermore, CA 94550.

Spectroscopic ellipsometers are used to determine spectral properties of surfaces (1) and thin films (2). Characteristics of different types of instruments have been compared by Aspnes (3). Most spectroscopic ellipsometers presently in use are of the non-compensating (photometric) type, employing a rotating analyzer (2,4,5), a rotating polarizer (6), or polarization modulation (7,8). Compensating ellipsometers, which are inherently more accurate (9) and do not require linear response of the photodetector (3) are mostly operated manually (10,11) at selected wavelengths, as had been done earlier (12,13). The present self-compensating spectral-scanning ellipsometer has resulted from extensive modification of a previously- built instrument (14) which had been based on principles proposed earlier (15). The design which has been used made it possible to combine the advantages of rapid spectral scanning with those of compensating measurements.

Optical Components

The ellipsometer employs the polarizer-compensator-sample-analyzer configuration, the arrangement of optical components is shown schematically in Fig. 1. Collimated monochromatic light is linearly polarized by a Glan-Thompson prism (polarizer). An achromatic quarter-wave retarder (compensator) produces elliptically polarized light incident on the sample surface. After reflection on the specimen, the light is linearly polarized and is extinguished by a second Glan-Thompson prism (analyzer). A photomultiplier tube is used to measure the intensity of the light transmitted by the analyzer, after collection by a second telescope. Azimuths of the transmission axes of polarizer and analyzer and the azimuth of the fast axis of the compensator are measured at compensation (extinction) and used to calculate the ellipsometer parameters, delta and psi (relative phase and amplitude).

The Faraday cells produce a magneto-optic rotation of the plane of polarization which is additive to the mechanical rotation of polarizer and analyzer prisms and is electronically controlled. The design of the solenoids has been reported before (14). Modulation currents of 10 kHz and 90 degree phase difference are applied to both Faraday cells, resulting in an oscillation of the effective polarizer and analyzer azimuths of 1-4 deg. p-p. Error signals derived from the response of the photomultiplier to about ten oscillations are generated by phase sensitive detection with integration and used to control bipolar operational amplifiers (±150 A) which drive the effective polarizer and analyzer azimuths to compensation. The fast response of the self-compensating circuit (slew rate for the Faraday cell rotation 1400 deg/s measured at 546.1 nm (16)) is essential for rapid spectral scanning.

Spectral scanning is achieved by rotating a continuously-variable interference filter, (17) positioned between a white light-source (75 W, current stabilized high-pressure Xe arc (18)) and the colimating telescope of the polarizer (Fig. 1). The maximum scan rate was 114 nm per second (1 pass through the spectral range every 3 seconds); lower noise levels can be achieved by use of a lower scan rate (23 nm per second or 1 pass through the spectral range every 15 seconds). The optical properties of this filter are given in Table I; as it revolves, the wavelength passed varies linearly from approximately 370 to 720 nm during the first half turn of rotation, and then decreased to 370 nm during the second half turn of rotation. A digital incremental encoder (19), which is coupled to the rotation shaft of the filter with a flexible linkage, is used to measure angular position and, thus, wavelength. Transmitted wavelength has been calibrated in terms of angular position with known spectral lines. At present, the useful spectral range is limited to about 410-700 nm

by the absorption of the Faraday cells in the UV and the sensitivity of the photomultiplier in the near IR. Advantages of the interference filter over other types of monochromators include high transmittance, straight-through beam path, small space requirement (2.5 cm), continuous bidirectional spectral scanning (no discontinuities in wavelength upon continuous rotation) and lack of polarization. Since the spectrum is scanned twice in opposite directions during a single revolution of the filter, some artefacts caused by filter imperfections or instrument response can be identified. The principal disadvantages of a continuously variable interference filter are the relatively broad bandwidth of the transmitted wavelength, (6 nm to 17 nm, see Table I) and the possible degradation of the filter coating with age.

The dependence of the specific rotation (effective Verdet coefficient, rotation per unit solenoid current) of the Faraday cells on wavelength has been determined experimentally and is shown in Fig. 3 for SF-6 glass cores, (1.91 cm diam., 15.24 cm length). Rotation of the analyzer and polarizer azimuths is linearly dependent on solenoid current over the entire dynamic range of the Faraday cells, which is ± 18° at 700 nm and ± 70° at 400 nm. Alternate glass cores listed in Table II have been used to provide better UV transmission but smaller rotation. All the glasses were annealed to reduce strain birefringence to less than 5×10^{-6} nm/m. A mechanical rotation of analyzer and polarizer prisms by use of stepping motors is initiated at the limits of the dynamic range of the Faraday cells, thus providing automatic operation of unlimited range.

A three-reflection Fresnel rhomb (20) with extremely low axial skew has been used as the achromatic quarterwave compensator.

It was found that the photomultiplier previously used for ellipsometry at a fixed wavelength of 546.1 (21) nm had to be replaced to avoid the loss of

signal in the red part of the spectrum. An "extended red" photomultiplier (22) greatly improved spectral scanning results. A gain-leveling circuit was incorporated into the Faraday cell controller to maintain wavelength-independent detector response, but its use was not normally required.

Computer System

The high rate at which ellipsometer data are generated during rapid spectral scanning requires the use of a digital data acquisition system shown schematically in Fig. 4. The current passed through the polarizer and analyzer Faraday cell solenoids to produce nulling are monitored by a microcomputer (23) over two channels of an 8-channel analog-to-digital converter. Faraday cell currents are converted post-experiment to analyzer and polarizer azimuths and, thus, ellipsometer parameters delta and psi under consideration of the wavelength-dependence of the effective Verdet coefficient. Wavelength, which varies linearly with the angular position of the filter, is monitored by counting pulses from the rotary incremental encoder. The encoder is interfaced to the computer via an addressable pulse counter. For each revolution the encoder generates an index pulse in one channel and 400 pulses in a second channel. Angular position is determined by counting the high-repetition pulses and using the index pulse to reset the count for every revolution; software interprets this count (0 to 400) as wavelength on the basis of calibrations. The frequency of the high-repetition pulses is used as a measure of scan rate.

Digital filtering is done by averaging all data collected between encoder pulses (1.7 nm spectral increment). Sampling of channels was limited by the A/D conversion rate (about 1000 readings per second). Further noise reduction is possible by averaging several scans.

Data are periodically transferred from the buffer memory to double density floppy disks (24) in unformatted form. To increase the storage efficiency of the disk, wavelengths are recorded in abbreviated form. Data can be displayed on the screen of a graphics terminal (25), as high-quality output from a digital interactive plotter (26), or as numeric output from a teletype (27). The graphics terminal also serves as the control console of the instrument.

Simulated spectral ellipsometer data for different optical film models are computed and displayed for comparison with measurements.

Applications

Spectroscopic ellipsometer measurements during the growth of lead deposits on a copper substrate are illustrated in Fig. 5. They show how the micromorphology of thin films can be determined (28). The spectral features of the substrate are still visible through a 31 nm thick layer obtained in the absence of dye, because this layer is highly porous, while the compact layer with the same metal content, obtained in the presence of a dye is optically opaque.

Wavelength-independent film properties of optical models such as film thickness and porosity, have been derived from spectral scans by treating measurements at different wavelengths as independent measurements. Thus, from a single spectral scan, by use of multi-dimensional data fitting, statistically-defined confidence intervals for such properties can be established (29).

The vastly increased information content of spectrascopic ellipsometer measurements compared to monochromatic measurements is illustrated in Fig. 6. Measurements for three films of different thickness are compared to simulations for a simple compact film model. It can be seen that at selected

wavelengths, agreement between model and measurement can be found, but this agreement does not extend over the entire spectral range, which it does for a more satisfactory model (28).

For the sake of brevity, only the relative phase parameter Δ is shown in the above examples. The relative amplitude parameter ψ, measured simultaneously, shows similar spectral variations.

The spectroscopic ellipsometer has also been used to study the adsorption of dyes on metal surfaces from aqueous solutions. Uniaxial, anisotropic, absorbing (dichroic) film models (30) have been used for deriving number density and orientation of adsorbed molecules (31).

Acknowledgment

This work was supported by the Director, Office of Energy Research, Office of Basic Energy Sciences, Materials Sciences Division of the U.S. Department of Energy under Contract No. DE-AC03-76SF00098.

References and Notes

1. E. T. Arakawa, T. Inagaki and M. W. Williams, Surf. Sci. 96, 248 (1980).

2. J. B. Theeten, Surf. Sci. 96, 275 (1980).

3. D. E. Aspnes in Optical Properties of Solids: New Developments, edited by B. O. Seraphin, North-Holland, Amsterdam 1976, p. 799.

4. D. E. Aspnes and A. A. Studna, Appl. Opt. 14, 220 (1975); SPIE Proc. 112 62 (1977); Rev. Sci. Instrum. 49, 291 (1978).

5. R. Kötz, B. Hayden, E. Schweizer and A. M. Bradshaw, Surf. Sci. 112, 229 (1981).

6. R. W. Stobie, B. Rao and M. J. Dignam, J. Opt. Soc. Am . 65, 25 (1975).

7. S. N. Jasperson and S. E. Schnatterly, Rev. Sci. Instrum. 40, 761 (1969); 41, 152 (1970).

8. V. M. Bermudez and V. M. Ritz, Appl. Opt. 17, 542 (1978).

9. D. E. Aspnes, Appl. Opt. 14, 1131 (1975).

10. B. Agius and J. Sieka, Rev. de Phys. Appliquée 12, 1171 (1977).

11. E. Idczak and E. Oleszkiewicz, Thin Solid Films 77, 301 (1981).

12. R. J. Archer, Phys. Rev. 110, 354 (1958).

13. C. L. McBee and J. Kruger, Surf. Sci. 16, 340 (1969).

14. H. J. Mathieu, D. E. McClure and R. H. Muller, Rev. Sci. Instrum., 45, 798 (1974).

15. H. P. Layer, Surf. Sci., 16, 177 (1969).

16. R. H. Muller and H. J. Mathieu, Appl. Opt. 13, 2222 (1974).

17. Optical Coatings Laboratory, continuously variable interference filter, VC-180-017.

18. Oriel, current-stabilized lamp power supply and housing C-72-20; Illumination Industries, Xenon Lamp X75-2002, 75 Watt.

19. Sensor Technology, incremental rotary encoder STRE-2014-010 with ADAC 1604/OPI-4 pulse counter.

20. Continental Optical, three-reflection Fresnal rhomb FAD-10, faces MgF_2-coated, entrance and exit beams coaxial with skew less than 0.01 deg.

21. RCA 931 A photomultiplier, range 300-650 nm, peak at 400 nm.

22. Hamamatsu R-928 photomultiplier, range 185-930 nm, peak at 400 nm.

23. Digital Equipment Corp., LSI-11/2 with central processor unit 975-64864, KEV-11 extended arithmetic chip, 32 k RAM add-on memory MSC-4601, 4-channel serial input-output board DLV-11, 4 channel 16 bit binary input pulse counter ADAC 1604/OPI, pulse controller board ADAC 1604/POC, 8-channel A to D converter, DATEL MST-LSI 2.

24. Dual floppy disk drive DSD 440 L11-2A.

25. Graphics terminal with hardcopy DEC VT 55.

26. Interactive digital plotter Tektronix 4662.

27. Teletype printer TT43, 300 BAUD.

28. Joseph C. Farmer and Rolf H. Muller, Electrochem. Soc. Meeting, San Francisco, CA, May 8-13, 1983, Ext. Abstr. 822, submitted to J. Electrochem. Soc.

29. Rolf H. Muller and Joseph C. Farmer, Intl. Conf. on Ellipsometry and other Optical Methods for Surface and Thin Film Analysis, Paris, June 7-10, 1983, Abstr. T-15, proceedings to be published in J. de Physique.

30. R.M.A. Azzam and N. M. Bashara, Ellipsometry and Polarized Light, North-Holland, Amsterdam, 1977, pp. 75, 356.

31. Manuscript in preparation.

32. Schott Optical Glass Technical Information No. 11, Schott Mainz, May 1976.

33. Schott Optical Glass Catalog, September 1, 1969.

Table I. Spectral Characteristics of the continuously variable interference filter monochromator (Optical Coatings Laboratory, Bonded CVF with 1 mm Slit)

Angular Position	Center Wavelength (1/2 PWR)	Wavelength Bandwidth (1/2 PWR)	Peak Transmission
degrees	nm	nm	percent
5	377.77	5.84	12.60
30	423.90	6.89	39.66
60	483.90	8.12	43.78
90	542.67	9.77	41.74
120	603.54	11.92	41.65
150	664.48	14.29	44.03
175	716.02	16.53	48.56
185	710.61	16.21	48.81
210	658.75	13.87	45.24
240	597.20	11.42	42.86
270	536.66	9.58	41.25
300	476.99	7.98	43.63
330	417.58	6.68	36.98
355	372.77	6.37	7.69

Table II. Properties of Faraday Cell Glass Cores (32,34).

Glass	Verdet Coefficient (min/Oe cm) at Wavelength, nm			Internal Transmittance (%) for 2.5 cm thickness at Wavelength, nm		
	450	500	600	370	400	440
BK 7	0.031	0.024	0.016	96	98.4	98.9
F 2	0.076	0.058	0.038	91	97	98.3
SF 2	0.085	0.065	0.043	85	97	99.0
SF 6	0.142	0.108	0.070	4	56	93

Figure Captions

Fig. 1. Spectral-scanning, self-nulling ellipsometer, optical components and electrical connections. 1. High pressure Xe lamp, 2 rotating interference filter, 3. collimator, 4. polarizer Glan-Thompson prism, 5. polarizer Faraday cell, 6. Fresnel rhomb achromatic retarder, 7. electrochemical cell, 8. analyzer Faraday cell, 9. analyzer Glan-Thompson prism, 10. collimator, 11. spectrally "flat" detector, 12. rotary incremental digital encoder, 13. spectral scanner drive motor.

Fig. 2. Circuits of self-compensating ellipsometer.

Fig. 3. Specific rotation and dynamic range of the polarizer Faraday Cells, with SF-6 glass cores (15.24 cm long) for wavelength 400 to 700 nm.

Fig. 4. Schematic of LSI-11/2 data acquisition and reduction system.

Fig. 5. Measured ellipsometer parameter delta for Pb deposits on Cu. Deposit thicknesses, 0 (bare substrate), 31, 60 and 110 nm based on charge passed. Deposition from 1 M $NaClO_4$, 0.005 M $Pb(NO_3)_2$, pH3 at -600 mV vs. Ag/AgCl. Dotted lines - no dye added, solid lines - 10 μM Rhodamine-B added.

Fig. 6. Spectroscopic simulations (solid lines) for compact Pb films of 0, 1, 5, 10, 20, 31, 60 and 110 nm on Cu and experimental measurements (dotted lines) for cathodic deposits of 31, 60 and 110 nm equivalent thickness (compact layer based on coulometric measurement of deposit).

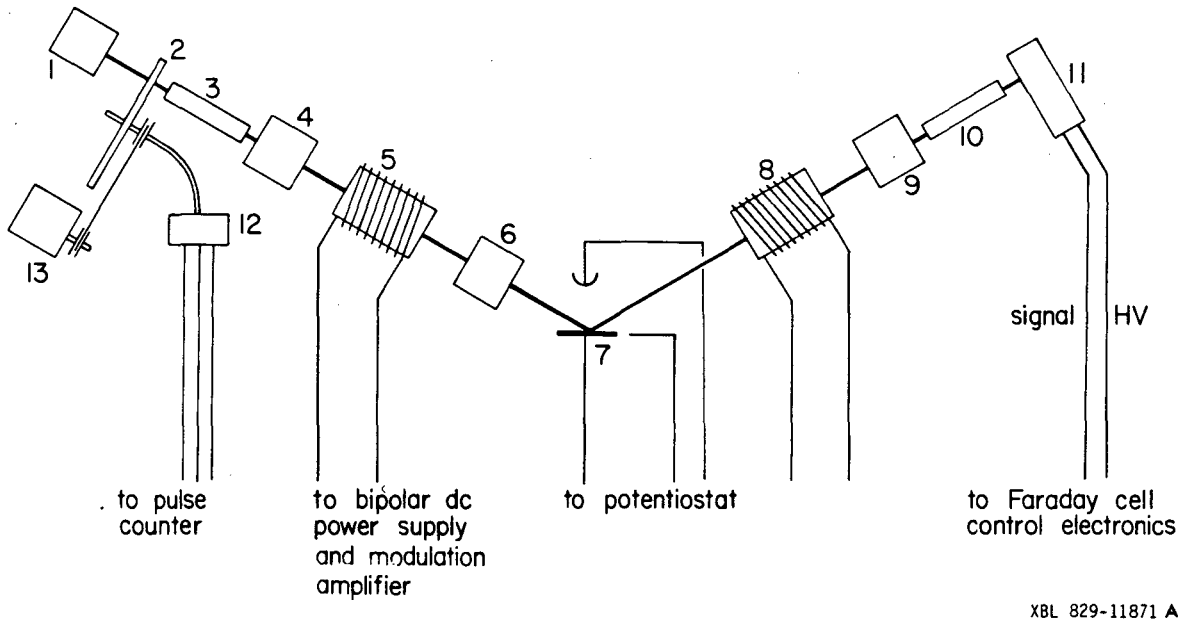
1
2
3
4
5
6
7
8
9
10
11
12
13
signal
HV
to pulse counter
to bipolar dc power supply and modulation amplifier
to potentiostat
to Faraday cell control electronics
XBL 829-11871 A

Fig. 1

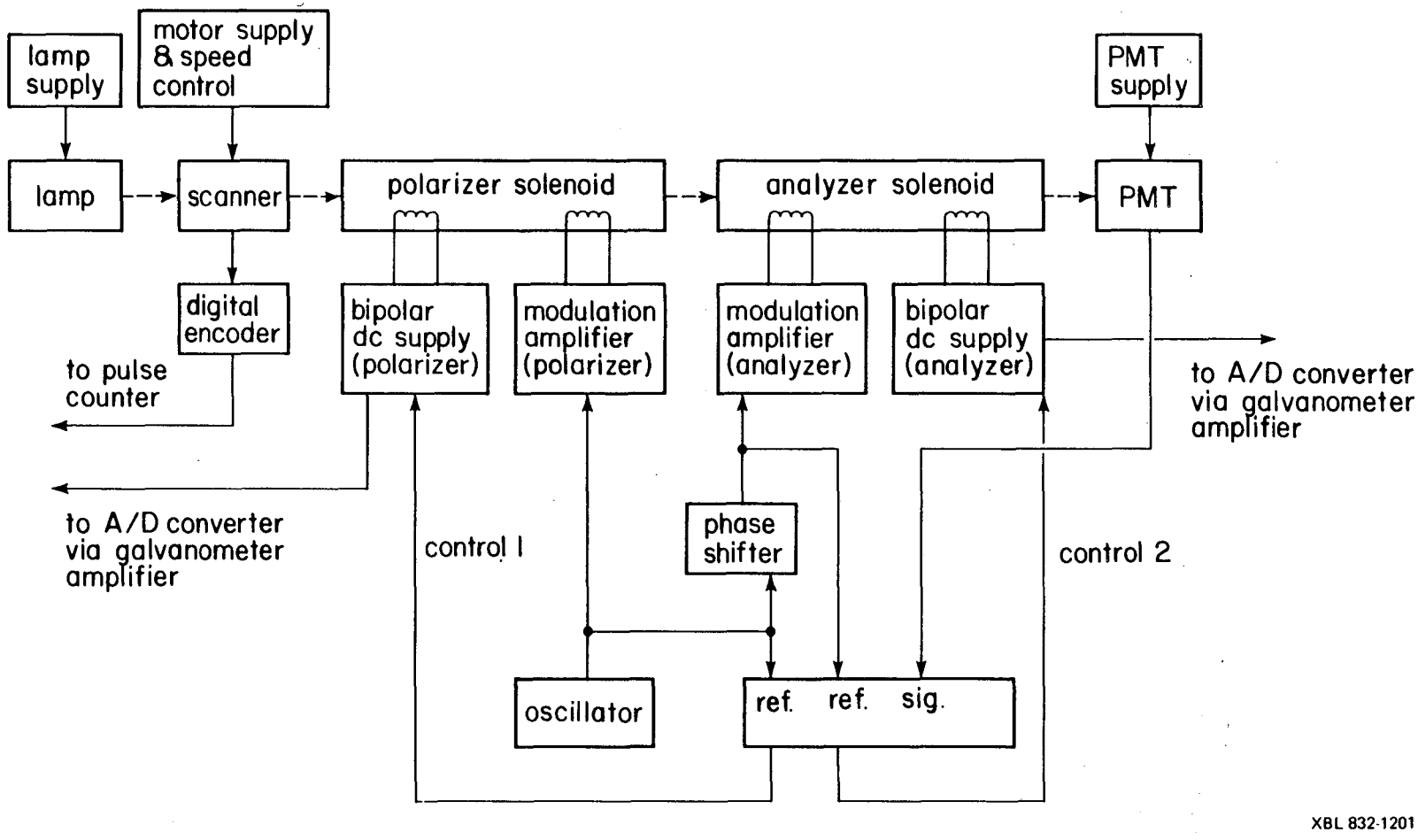
lamp supply
motor supply & speed control
PMT supply
lamp
scanner
polarizer solenoid
analyzer solenoid
PMT
digital encoder
bipolar dc supply (polarizer)
modulation amplifier (polarizer)
modulation amplifier (analyzer)
bipolar dc supply (analyzer)
to pulse counter
to A/D converter via galvanometer amplifier
to A/D converter via galvanometer amplifier
control 1
phase shifter
control 2
oscillator
ref. ref. sig.
XBL 832-1201

Fig. 2

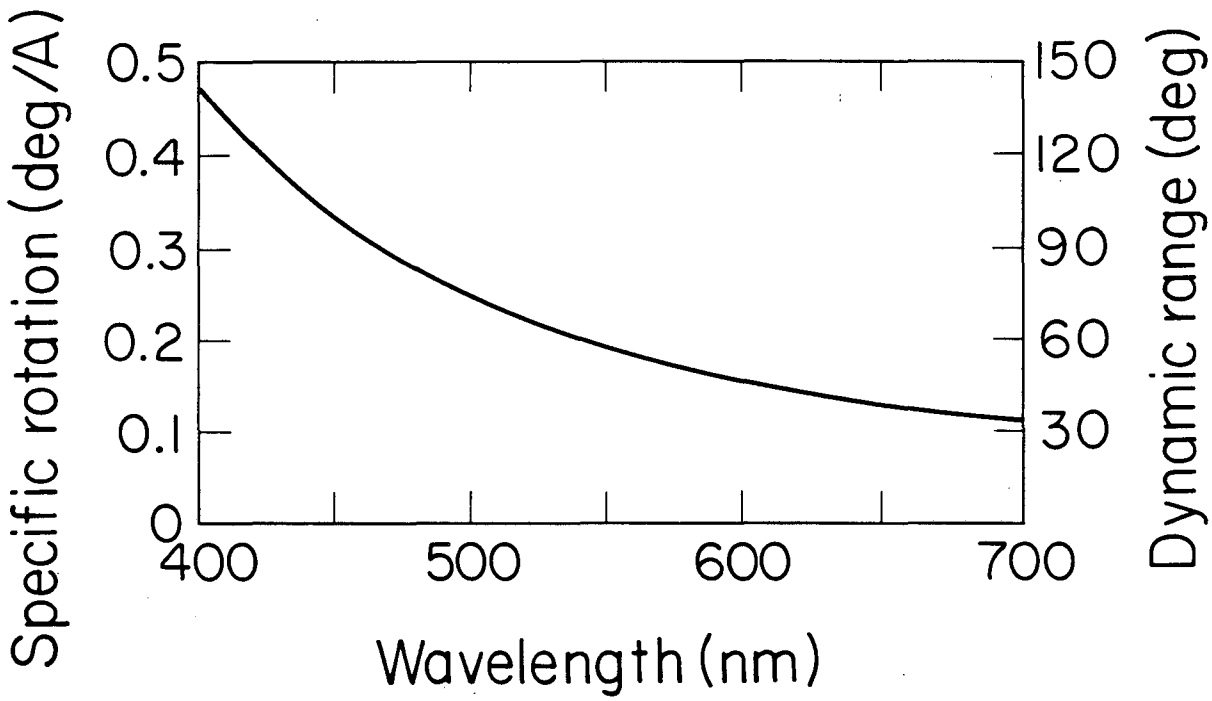

XBL 834-1202B

Fig. 3

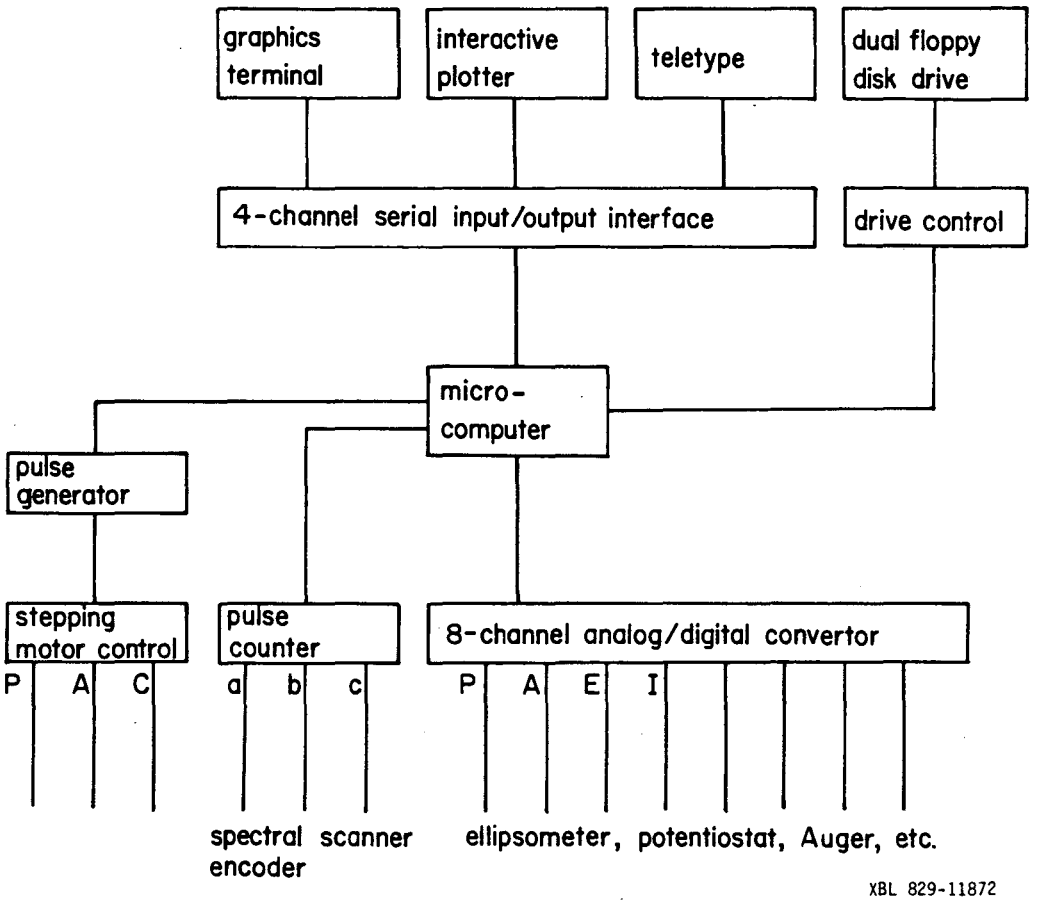
graphics terminal
interactive plotter
teletype
dual floppy disk drive
4-channel serial input/output interface
drive control
micro-computer
pulse generator
stepping motor control
P
A
C
pulse counter
a
b
c
8-channel analog/digital convertor
P
A
E
I
spectral scanner encoder
ellipsometer, potentiostat, Auger, etc.
XBL 829-11872

Fig. 4

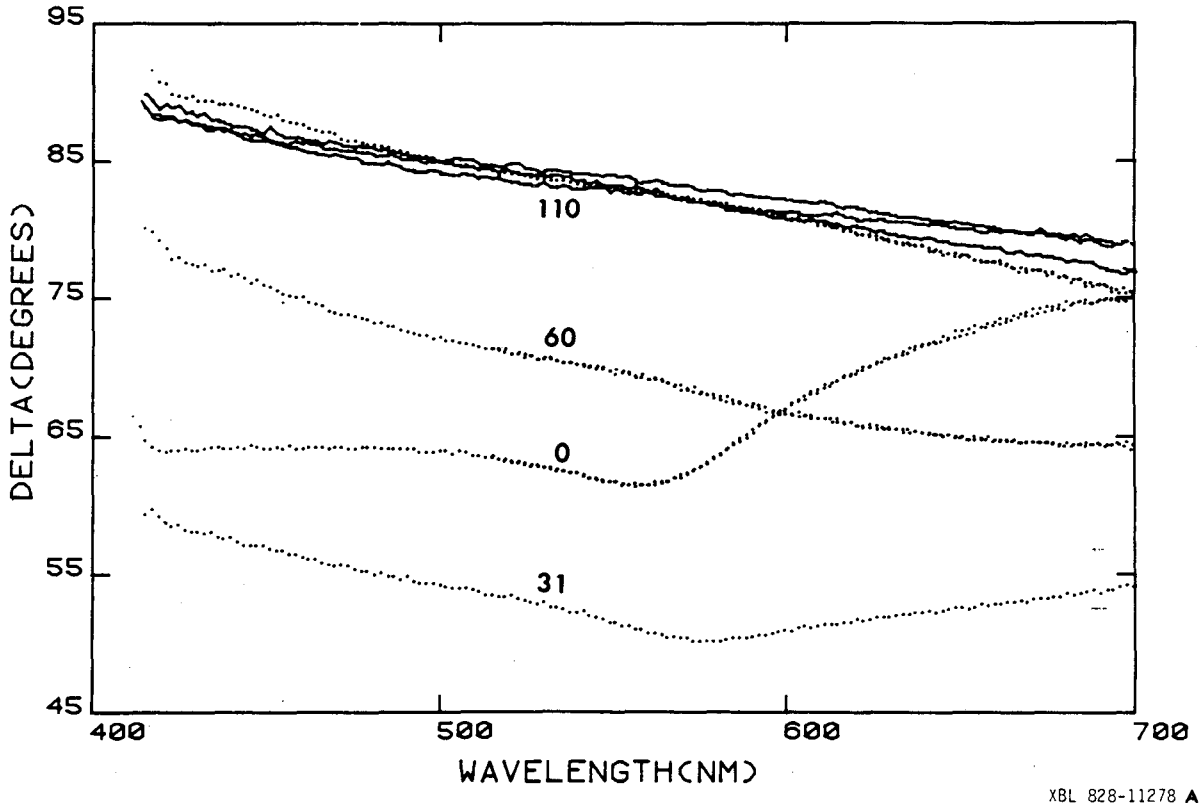
95
85
75
65
55
45
DELTA(DEGREES)
110
60
0
31
400
500
600
700
WAVELENGTH(NM)
XBL 828-11278 A

Fig. 5

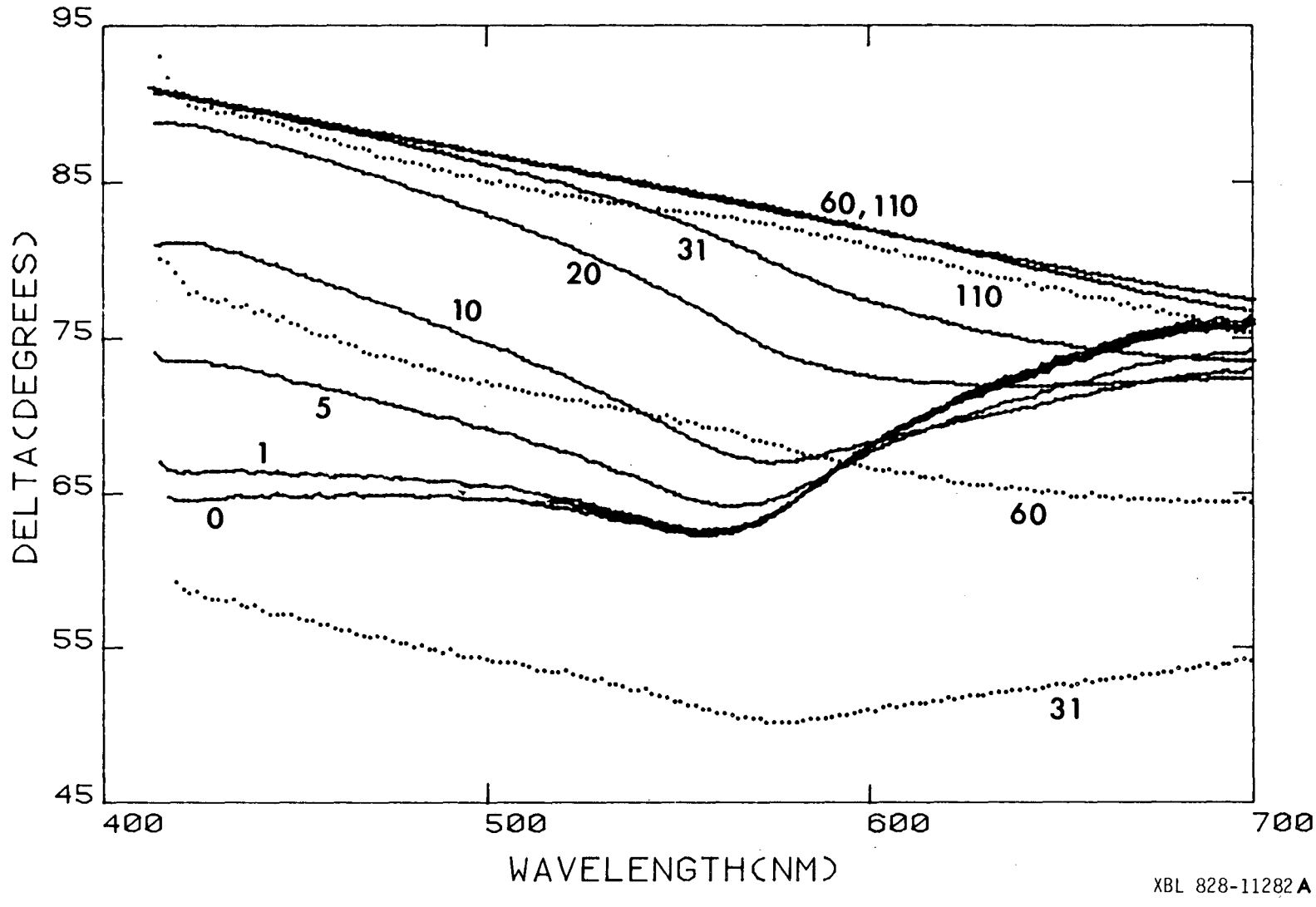
95
85
75
65
55
45
DELTA(DEGREES)
400
500
600
700
WAVELENGTH(NM)
60, 110
31
20
110
10
5
1
0
60
31
XBL 828-11282A

Fig. 6

This report was done with support from the Department of Energy. Any conclusions or opinions expressed in this report represent solely those of the author(s) and not necessarily those of The Regents of the University of California, the Lawrence Berkeley Laboratory or the Department of Energy.

Reference to a company or product name does not imply approval or recommendation of the product by the University of California or the U.S. Department of Energy to the exclusion of others that may be suitable.

TECHNICAL INFORMATION DEPARTMENT
LAWRENCE BERKELEY LABORATORY
UNIVERSITY OF CALIFORNIA
BERKELEY, CALIFORNIA 94720